



HAL
open science

Towards a better understanding of the flocculation/flotation mechanism of the marine microalgae *Phaeodactylum tricornutum* under increased pH using atomic force microscopy

Cécile Formosa-Dague, Vincent Gernigon, Mickaël Castelain, Fayza Daboussi, Pascal Guiraud

► To cite this version:

Cécile Formosa-Dague, Vincent Gernigon, Mickaël Castelain, Fayza Daboussi, Pascal Guiraud. Towards a better understanding of the flocculation/flotation mechanism of the marine microalgae *Phaeodactylum tricornutum* under increased pH using atomic force microscopy. *Algal Research - Biomass, Biofuels and Bioproducts*, 2018, 33, pp.369-378. 10.1016/j.algal.2018.06.010 . hal-01886487

HAL Id: hal-01886487

<https://hal.science/hal-01886487>

Submitted on 13 Jan 2022

HAL is a multi-disciplinary open access archive for the deposit and dissemination of scientific research documents, whether they are published or not. The documents may come from teaching and research institutions in France or abroad, or from public or private research centers.

L'archive ouverte pluridisciplinaire **HAL**, est destinée au dépôt et à la diffusion de documents scientifiques de niveau recherche, publiés ou non, émanant des établissements d'enseignement et de recherche français ou étrangers, des laboratoires publics ou privés.



Towards a better understanding of the flocculation/flotation mechanism of the marine microalgae *Phaeodactylum tricornutum* under increased pH using atomic force microscopy

C. Formosa-Dague^{a,b,c,*}, V. Gernigon^a, M. Castelain^{a,c}, F. Daboussi^a, P. Guiraud^{a,c}

^a LISBP, Université de Toulouse, INSA, INRA, CNRS, Toulouse, France

^b LAAS-CNRS, Université de Toulouse, CNRS, Toulouse, France

^c Fédération de Recherche FERMAT, CNRS, Toulouse, France

ARTICLE INFO

Keywords:

Phaeodactylum tricornutum
Flocculation
Flotation
Atomic force microscopy
Biophysics

ABSTRACT

In the context of climate change, the interest for sustainable sources to produce energy is growing. One promising resource for biofuel production is microalgae, but their industrial use is limited by the lack of efficient harvesting techniques. In this study, we use a multi-scale approach to understand the magnesium hydroxide-mediated flocculation/flotation mechanism of *Phaeodactylum tricornutum*, an effective oil-producer diatom, under high pH. While flotation experiments give a population-scale quantification of the efficiency of flocculation/flotation using magnesium or calcium hydroxide, or at increased pH, AFM allows probing the mechanical properties of the cells at different pH values. Finally we develop an original strategy to functionalize AFM tips with hydroxide particles that we use in multiparametric imaging experiments to understand at the molecular scale the forces driving the adhesion of hydroxide particles to cells. Altogether, our results give a better understanding of the molecular mechanism underlying alkaline flocculation/flotation, paving the way towards the development of low-cost flocculant-free flotation harvesting processes.

1. Introduction

The group of diatoms, which comprises from 10,000 to 100,000 different species, making them the second most diverse group of photosynthetic organisms, is responsible for 40% of marine primary productivity [1, 2]. Among the diatoms that have attracted attention so far, *Phaeodactylum tricornutum* stands out because of its natural abundance in particular omega-3 eicosapentaenoic acid (EPA), pigments and antioxidants [3–5]. Today, *P. tricornutum* is mainly exploited for aquaculture and nutraceutical applications. But because of its ability to produce up to 45% of lipids, *P. tricornutum* presents a high potential in biofuel production, although for this particular purpose genetic engineering is required to modify the quantity [6] and characteristics of the produced fatty acids in regards to their usage as biofuel feedstock [7]. Moreover, the use of biofuels as an alternative to fossil fuels is at the moment, technically not feasible [5].

Indeed, while small-scale production of *P. tricornutum* to obtain high value-added molecules is efficient, the large-scale production from microalgae of molecules substituting fossil carbon resources faces a number of technical challenges that have made the current growth and development of the biofuel industry economically unviable [8]. The

main limitation encountered by industrials is the harvesting of microalgae [9]. Harvesting consists in removing at a minimal cost the microalgae from their aqueous culture medium, where their concentration is low (0.3–3 g/L) [10], while keeping their cell wall intact not to lose their precious production in solution. This crucial step of harvesting and dewatering has been assumed to account for one third of the entire price of microalgal biomass production in industrial processes [11]. Several methods have been proposed for algae harvesting, including centrifugation, filtration, flocculation, sedimentation and flotation [12]. However, most of these methods present high costs and energy consumption, for low efficiency rates. Centrifugation for example consumes a large amount of electricity and causes damage to the cells because of the high shear forces, while filtration costs are increased by the clogging of membranes inevitable with unicellular small cells such as microalgae [13].

In this context, flotation that takes advantage of algae's natural characteristics of relatively low density and self-floating tendency, appears to be the most promising harvesting technique [14]. Assisted flotation consists in air or gas bubbles rising in a microalgal suspension. As a result, microalgae cells get attached to bubbles interfaces and are carried out and accumulated on the suspension surface [12]. It is a

* Corresponding author at: LISBP, INSA de Toulouse, 135 avenue de Rangeuil, 31077 Toulouse Cedex 4, France.
E-mail address: formosa@insa-toulouse.fr (C. Formosa-Dague).

relatively rapid operation that needs low space, has moderate operational costs, and that could thus overcome the bottleneck of feasible microalgal biofuel production [13]. However important factors can affect microalgal flotation, such as the charge of the surface of the cells. The surface of microalgae present a negative surface charge; the surface of bubble in an aqueous medium being also negatively charged [15], the microalgal surface interaction with bubbles is then repulsive, which prevents adhesion, and therefore capture and flotation. Thus to improve flotation efficiency, chemical flocculants are added to the algal suspension to aggregate cells into large flocs that can then be easily separated from the water by further flotation [16]. However addition of these molecules might not be an ideal solution because of their potential toxicity on the algal biomass if it is used for food for example, as well as in the recycled water [17]. Therefore in many cases auto-flocculation would be a preferred alternative to improve water separation by flotation. There are several known auto-flocculation mechanisms, among which one is based on the precipitation of magnesium ions at high pH [18]. This mechanism has been described already for microalgal species such as *Dunaliella salina* [19], *Chlorella vulgaris* [20], *Nannochloropsis oculata* [20], but also for *P. tricornutum*. Indeed, in recent publications, it has been showed that flocculation of *P. tricornutum* induced by an increase of pH in marine water, was the result of the precipitation of magnesium ions into magnesium hydroxide presenting a positively charged surface and thus flocculating the cells through a charge neutralization mechanism [20, 21]. However, for the moment, there are no evidence nor characterization of the interactions between cells and magnesium hydroxide that could confirm or complement the information on this mechanism. Also, the effects of an increasing pH on cells were never investigated, as surface modification of the cells at such pH could participate in the flocculation/flotation mechanism.

It is now possible to answer such questions thanks to recent advances in atomic force microscopy (AFM) techniques. AFM, first developed in 1986 [22], is a technology particularly well suited for the study of living microorganisms, as it features high-resolution imaging capabilities and is able to operate in liquid. Furthermore, it is also a highly sensitive force machine, able to record forces as small as 20 pN in force spectroscopy mode, making it then possible for researchers to gain insights into the mechanical properties and molecular interactions of single cells [23]. Recently new force-spectroscopy based techniques were developed, such as multiparametric imaging that offers the possibility to image the surface structure of living cells, while mapping their adhesive properties at high spatial resolution [24–26]. Furthermore, AFM tips used to perform experiments can also be functionalized with particles [27] for example, and thus provide a way to understand and characterize the interaction forces between cells and these particles.

In this study, we use a multi-scale approach to understand the magnesium hydroxide-mediated flocculation/flotation mechanism of *P. tricornutum* cells under high pH. For that, we first perform flotation tests, which give a population-scale quantification of the efficiency of magnesium hydroxide as a flocculant; we also evaluate the effects of another hydroxide that can also form in marine water at high pH; calcium hydroxide. We then go down to the micro-scale and use AFM to image and probe the mechanical properties of living *P. tricornutum* cells at different pH values in order to understand the effects of increasing pH on their surface properties. We finally develop an original strategy to functionalize AFM tips with hydroxide particles that we use in multiparametric imaging experiments to understand at the molecular scale the forces driving the adhesion between these hydroxides and the cells. Altogether, our results allow giving a better understanding of the mechanisms underlying alkaline flocculation/flotation, and show that not only the precipitates are responsible for the formation of flocs and the further separation by flotation, but also the cells and the structural changes they undergo at high pH. Such information may have important impacts on the development of low-cost flocculants-free

flotation processes, and thus on the further use of these processes in relevant biotechnological applications to decrease costs.

2. Material and methods

2.1. Strain and culture conditions

Phaeodactylum tricornutum strain CCMP2561 (Bigelow National Center for Marine Algae and Microbiota) was grown in synthetic Sea Salts (40 g/L, Sigma S9883) containing filtered Guillard f/2 medium [28] (Sigma G0154) without silica, at 20 °C, under agitation (100 rpm), in 75 mL non-coated culture flasks (15 mL of culture), 500 mL non-coated culture flasks (150 mL of culture), and 2 L Erlenmeyer (500 mL of culture). The incubator was equipped with white neon light tubes providing illumination of 120 $\mu\text{mol photons m}^{-2}\text{s}^{-1}$ with a photoperiod of 12 h light:12 h dark. All experiments in the study were performed in Sorbitol buffer 375 mM at pH = 8 or pH = 10. For that, cells were harvested by centrifugation (3000 rpm, 10 min) and washed two times in sorbitol buffer 375 mM at pH = 8 or pH = 10.

2.2. Dry weight concentration determination

Glass fiber filters (0.45 μm , Whatman GF6) were first dried at 105 °C for 24 h; their initial mass was measured after drying. *P. tricornutum* cells were harvested by centrifugation (3000 rpm, 10 min) and washed two times in sorbitol buffer 375 mM at pH = 8 or pH = 10. Then 50 mL of the cell suspension was filtered on the dried filters, which were then allowed to dry for 24 more hours at 105 °C. Filters were finally weighed again: the weight difference before and after filtration of the cell suspension corresponds to the dry mass of the filtered cells. Knowing the volume of the initial cell suspension, the concentration can be obtained.

2.3. Flotation experiments

Dissolved air flotation (DAF) experiments were achieved in a Multiplace Orchidis™ Flottatest, as described previously [19]. Algal suspensions of 500 mL, at a biomass dry concentration comprised between 0.3 and 0.4 g/L, were harvested by centrifugation (3000 rpm, 10 min), washed two times in sorbitol buffer 375 mM at pH = 8 or pH = 10, and added to flotation-test beakers. The depressurization at atmospheric pressure of sorbitol buffer 375 mM at pH = 8 or pH = 10 and saturated by air at 6 bars induced the formation of bubbles. Sorbitol buffer free of algae was pressurized for 30 min before injection into the beakers. The injection was controlled by a solenoid valve and 100 mL of pressurized sorbitol buffer was added to each beaker sample. Flotation tests were conducted in the presence or not of a flocculant; here Mg(OH)₂ or Ca(OH)₂. Tests with no flocculant were performed in sorbitol buffer at pH = 8 or pH = 10, whereas tests using Mg(OH)₂ or Ca(OH)₂ were performed in sorbitol buffer at pH = 10 to avoid dissolution of the hydroxides. In these cases, before depressurization, hydroxides were added at a final concentration of 10.5 mM for Ca(OH)₂ and of 5.7 mM, 14.3 mM or 57 mM for Mg(OH)₂ in the flotation-test beakers containing the algal suspensions in buffer. Mechanical mixing (100 rpm, 5 min) allowed homogenization of the suspension. Note that in our conditions, the hydroxide particles are bigger than if they were directly formed *in situ*, thus their specific surface is smaller, and concentrations higher than in physiological conditions are used. To evaluate the efficiency of flotation tests, KOVA counting slides were used. For each test, 10 samples of the algal suspension withdrawn in the middle of the suspension, before and 10 min after the depressurization, were used for counting and determine the cell concentration. The percentage of efficiency corresponds to the percentage of cells removed for the algal suspension after flotation.

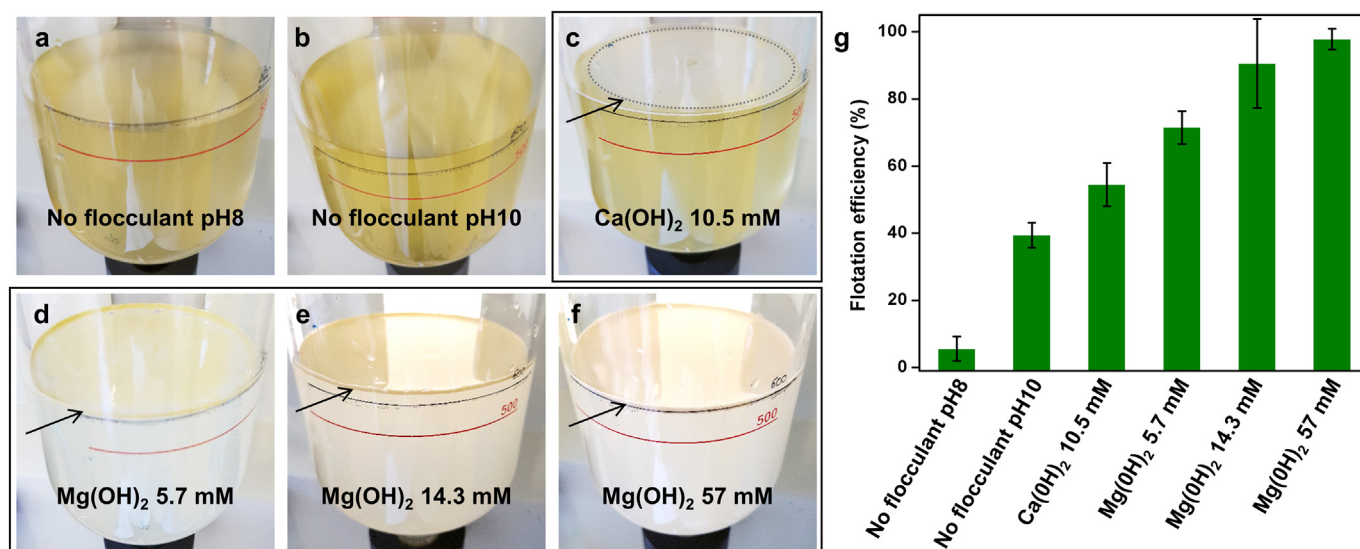


Fig. 1. Flotation of *Phaeodactylum tricornutum*. (a) Pictures of the resulting cell suspension after flotation of *P. tricornutum* cells in sorbitol buffer with no flocculant at pH = 8 or (b) pH = 10. (c) Resulting cake after flotation in sorbitol buffer at pH = 10 with Ca(OH)₂ at a concentration of 10.5 mM (indicated by the black arrow and the dotted circle) or (d) Mg(OH)₂ at a concentration of 5.7 mM, (e) 14.3 mM and (f) 57 mM (indicated by the black arrows). (g) Histogram representing the flotation efficiency in % in the different flotation conditions. For each condition, experiments were conducted twice, with a microalgal biomass dry weight comprised between 0.3 and 0.4 g/L.

2.4. Optical imaging

The optical images of *P. tricornutum* cells before and after flotation experiments were directly obtained by sampling 1 mL of the cell suspension or of the cake obtained after flotation. These samples were then deposited on glass surfaces and allowed to stand for 30 min at room temperature. Images were recorded at high magnification ($\times 50$) using an inverted Axio Observer Z1 microscope (Zeiss).

2.5. Zeta potential measurements

The global electrical properties of *P. tricornutum* cell surface were assessed by measuring the electrophoretic mobility which corresponds to the velocity of suspended cells exposed to an electric field. To this end, microalgae were harvested by centrifugation (3000 rpm, 10 min), washed two times in sorbitol buffer 375 mM at pH = 8 or pH = 10 and resuspended in the same solution at a final concentration of 1.5×10^6 cell/mL. The electrophoretic mobility was then measured using an automated laser zetameter (Zetasizer NanoZS, Malvern Instruments). For each condition, cells coming from 3 independent cultures were analyzed.

2.6. AFM imaging and force spectroscopy experiments

Before AFM experiments, cells were harvested by centrifugation (3000 rpm, 10 min) and washed two times in sorbitol buffer 375 mM at pH = 8 or pH = 10. Cells were then immobilized on polyethylenimine (PEI, Sigma P3143) coated glass slide prepared as previously described [29]. Briefly, freshly oxygen activated glass slides were covered by a 0.2% PEI solution in deionized water and left for incubation overnight. Then the glass slides were rinsed with deionized water and dried under nitrogen. A total of 1 mL of cell suspension was then deposited on the PEI slides, allowed to stand for 30 min at room temperature, and rinsed with sorbitol buffer 375 mM at pH = 8 or pH = 10. Images were recorded in sorbitol buffer at pH = 8 or pH = 10 using the Quantitative Imaging™ mode available on the Nanowizard III AFM (JPK Instruments, Berlin, Germany). Multiparametric images were recorded with MLCT AUWH cantilevers (Bruker, nominal spring constant of 0.01 N/m) using an applied force of 0.7 nN, a constant approach/retract speed of 90 $\mu\text{m/s}$,

and a z-range of 2 μm . For nanoindentation experiments, the applied force was comprised between 1 and 5 nN depending on the condition with MLCT AUWH cantilevers with nominal spring constants comprised between 0.01 N/m and 30 N/m. Young's moduli were then calculated from 80 nm indentation curves using the Hertz model [30] in which the force F , indentation (δ) and Young's modulus (Y_m) follow the equation $F = (2 \times Y_m \times \tan\alpha) / (\pi \times (1 - \nu^2) \times \delta^2)$, where α is the tip opening angle (17.5°), and ν the Poisson ratio (arbitrarily assumed to be 0.5). Finally force spectroscopy experiments, MLCT AUWH cantilevers with a nominal spring constant of 0.01 N/m, functionalized with hydroxides or not, were used at a constant applied force of 0.25 nN. The cantilevers spring constants were determined using the thermal noise method [31] before each experiment.

2.7. AFM tip functionalization with hydroxides

To prepare functionalized AFM with Ca(OH)₂ and Mg(OH)₂, MLCT AUWH tips were first dipped into a thin layer of UV-curable glue (NOA63, Norland Edmund Optics), then into a thin layer Ca(OH)₂ or Mg(OH)₂ particles deposited on a glass slide. Functionalized tips were then put under UV-light for 10 min to allow the glue to cure.

2.8. Scanning electron microscopy imaging of AFM tips

AFM cantilevers with tips functionalized or not were first carbonated and then imaged using a Jeol 6400 electron microscope (Jeol, Tokyo, Japan) equipped with an EDS Bruker SDD detector, at an acceleration voltage of 20 kV. Energy-Dispersive X-ray (EDX) analysis was also performed in order to obtain the atomic concentrations of Mg and Ca in particular present in each sample imaged.

3. Results

3.1. Both pH increase and hydroxide-mediated flocculation improve flotation efficiency

We first studied at the population scale the efficiency of *P. tricornutum* separation by flotation (Fig. 1). Fig. 1a to f are pictures of the resulting algae suspensions after flotation or after flocculation/

flotation. In each case, experiments were conducted in salt-free buffer (sorbitol 375 mM) so to evaluate the effects of each parameter, pH increase or addition of hydroxides, independently. When magnesium or calcium hydroxides were used, the pH of the buffer was set to 10, to prevent their dissolution at lower pH. When no flocculants were used, we can see from the pictures that cells did not form agglomerates at the surface even though at high pH the flotation was efficient at 39.4%, meaning that 39.4% of the cells were moved to the surface by the air bubbles (Fig. 1a, b and g). Addition of $\text{Ca}(\text{OH})_2$ in the algal suspension at the maximum concentration that could be found in our synthetic marine water (10.5 mM), caused the cells to agglomerate. After flotation, these agglomerates that were moved to the surface by the bubbles, could be directly visualized (Fig. 1c). Addition of $\text{Mg}(\text{OH})_2$ at increasing concentrations also led to the formation of cell agglomerates, also visible at the surface of the suspensions after flotation (Fig. 1d to f). Concerning flotation efficiencies (Fig. 1g), flocculation using $\text{Ca}(\text{OH})_2$ resulted in a flotation efficiency of 54.5%, while a smaller concentration of $\text{Mg}(\text{OH})_2$ allowed better separating the cells from the water (efficiency of 71.5% using 5.7 mM of $\text{Mg}(\text{OH})_2$). With higher $\text{Mg}(\text{OH})_2$ concentrations, until 57 mM (maximum reachable concentration in our synthetic marine water), a flotation efficiency of almost 100% was reached (90.6% with 14.3 mM and 97.8% with 57 mM), meaning that almost all the cells were removed from the water and agglomerated at the surface. These experiments then allowed to show that increasing the pH in the algae suspension without adding any flocculants was enough to increase flotation efficiency, and that magnesium hydroxide is a better flocculant than calcium hydroxide, allowing to reach higher separation rates, in our experimental conditions. Thus at this stage, two questions can be asked: (i) why does a pH of 10 allow increasing flotation efficiency and (ii) why is magnesium hydroxide a better flocculant than calcium hydroxide in our experimental conditions?

3.2. Increasing the pH modifies the surface properties of *P. tricornutum*

In order to bring information which could help answering the first question, we investigated the influence of a pH of 8 (pH in the culture medium), and of 10 on the micro-scale biophysical properties of the cell surface. To this end, two techniques to characterize the cell surface were used; AFM and zeta potential measurements. Fig. 2a presents AFM height images of living *P. tricornutum* cells in sorbitol buffer at a pH of 8, close to the one found in our culture conditions, and at a pH of 10. On these images, pH increase does not seem to affect cell morphology, which is further confirmed by the length, width and height measurements that were performed on at least 10 cells in both conditions, and presented in Fig. 2b. This confirms that the buffer we are using, containing 375 mM of sorbitol, does not cause osmotic pressure on the cells. However, concerning the surface charge of the cells, zeta potential measurements (Fig. 2c) showed that increasing the pH in the buffer used for experiments led to an increase of the electronegativity of the cell surface, from -18.9 ± 3.4 mV at pH = 8 to -27.1 ± 3.2 mV at pH = 10 (mean \pm SD from 15 measurements at each pH), most likely resulting from an ionization of the hydroxyls functions present on the polysaccharides ($\text{pK}_a > 10$, [32]) that composes for one third the cell wall of *P. tricornutum* [33]. But the major change that cell surface experiences at a pH of 10 concerns the nanomechanical properties. To obtain quantitative information on these properties, we determined the Young modulus (Y_m) of the microalgae cells through nanoindentation measurements, in buffer at the two different pHs (Fig. 2d to f). In this type of measurements, the cantilever, which mechanical properties are known, is pressed against the cells at a given force. This allow extracting the Y_m of the cell wall, a parameter that reflects its resistance to compression (the higher the Young modulus value, the stiffer the cell wall). Y_m values are obtained first by converting force curves into force vs indentation curves, showed in Fig. 2e, and second by analyzing these curves with a theoretical model, in our case, the Hertz model (black empty circles on the curves in Fig. 2e). As showed in the AFM image in

Fig. 2d, local nanoindentation measurements were performed on areas of $1 \mu\text{m} \times 1 \mu\text{m}$ on the center and on the side of the cells. The indentation curves recorded (Fig. 2e) showed that in both cases, there was a difference in the indentation between the center and the side of the cells, most probably due to the presence in the center of the chloroplast and of the lipid droplet that *P. tricornutum* produces. Another information that could be extracted from these curves is that the AFM probe was able to indent deeper in cells at pH = 8 than at pH = 10, leading thus to the conclusion that increasing pH also increases the rigidity of the cell wall. Quantitative measurements, presented in Fig. 2f, confirmed these information; cell side at a pH of 8 presented a Y_m of 249 ± 153 kPa, that was more than two-times increased in the center (580 ± 294 kPa, mean \pm SD on a total of $n = 8192$ curves from 8 different cells), in line with previous nanomechanical measurements [29]. At increased pH, cells were significantly more rigid even though Y_m values showed a high heterogeneity (p value < 0.05 , unpaired t -test), with a Y_m of 4324 ± 2079 kPa on the center and of 2951 ± 1251 kPa on the side of the cells (mean \pm SD on a total of $n = 8192$ curves from 8 different cells). Thus, although intracellular structures caused a local increase in the rigidity of the above probed cell wall, these results show that with increasing the pH, the cell wall undergoes a deep remodeling that is reflected by an increased rigidity. This result, when put in parallel with the flotation efficiencies obtained in the absence of flocculant, seems to indicate that perhaps the deformability capacity of the cells is involved in their interactions with bubbles.

3.3. Magnesium hydroxide interacts and adheres to the surface of the *P. tricornutum* cells

To address the second question that rose from flotation experiments, why does magnesium hydroxide seem to be a better flocculant than calcium hydroxide, we decided to take a closer look, at the micrometer-scale, at the cells present at the surface of the suspensions after flotation or flocculation/flotation. To this end, these cells were used for both optical and AFM imaging (Fig. 3). Fig. 3a, d and g show that in the absence of flocculant, at a pH of 10, cells did not present any particularities, and their surface was smooth, as it can be seen on the cross-section in Fig. 3g. However, after flotation using 5.7 mM of $\text{Mg}(\text{OH})_2$ as a flocculant, optical imaging showed that cells were covered by hydroxides particles (Fig. 3b). This observation was then confirmed by AFM data that indeed revealed the presence of hydroxide particles directly adhered on the surface of the cells (Fig. 3e and h). In the case where $\text{Ca}(\text{OH})_2$ was used to flocculate the cells, we can see that only a few hydroxide particles were adhered to the cells, thus leading to think that $\text{Mg}(\text{OH})_2$ is a better flocculant because it seems to bind the cells more efficiently than calcium hydroxide. However this hypothesis needs to be confirmed.

3.4. Force measurements uncover the mechanical strength of hydroxide binding to *P. tricornutum* cells

In order to evaluate the binding efficiencies of magnesium and calcium hydroxides to cells, we chose to develop a new strategy to directly functionalize AFM tips with these hydroxides. The method is presented in Fig. 4a to c. Inspired by studies where micro-sized particles or nanoparticles were glued to AFM cantilevers or tips [27, 34], we chose to directly functionalize silicon nitride AFM tips with hydroxide particles using a UV-curable glue. The protocol that we used for that, described in the material and methods section (paragraph 2.7), is depicted in Fig. 4a, b and c. Then, to confirm their good functionalization, bare and modified tips were analyzed using scanning electron microscopy (SEM) imaging and energy-dispersive X-ray (EDX). The results obtained, presented in Fig. 4d to f, showed that particles were indeed present on the tip after functionalization. The atomic concentration spectra further confirmed that the particles observed were indeed

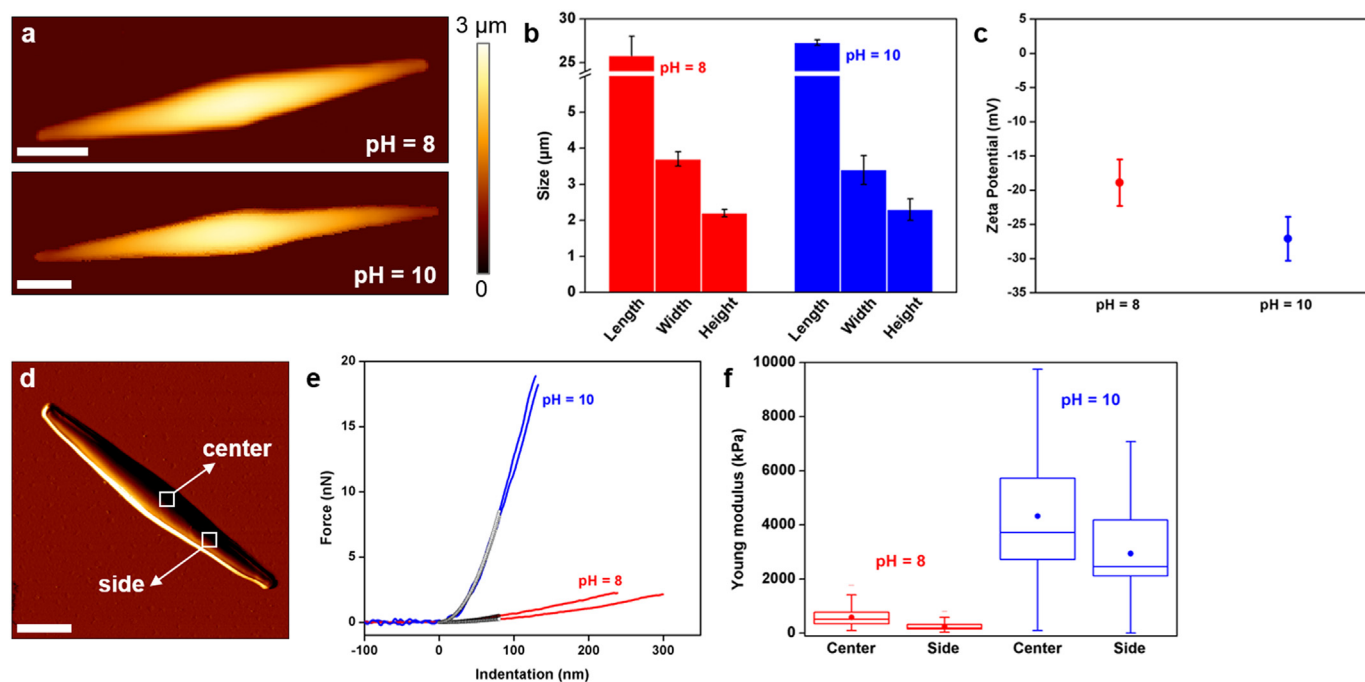


Fig. 2. Morphology and surface properties of cells at different pH. (a) AFM height images of *P. tricornutum* cells in sorbitol buffer at pH = 8 or pH = 10. (b) Histogram representing the length, width and height of cells at pH = 8 or pH = 10. For each conditions, 6 cells coming from 2 independent cultures were analyzed. (c) Zeta potential of cells in sorbitol buffer as a function of the pH. For each pH, 15 independent measurements were performed. (d) AFM vertical deflection image of a single *P. tricornutum* cells in sorbitol buffer at pH = 10. Squares indicate 1 μm × 1 μm areas where local nano-indentation measurements were performed. (e) Representative indentation curves recorded on the center or the side of cells at pH = 8 or pH = 10. Black empty circles on the curves represent the Hertz model used to fit the curves and extract the Young modulus values (f) Box charts showing the distribution of Young modulus values obtained from curves recorded on the center or the side of cells in sorbitol buffer at pH = 8 or pH = 10. For each condition, 8192 curves recorded on 8 cells coming from 3 independent cultures were analyzed. Scale-bars in AFM images correspond to 5 μm.

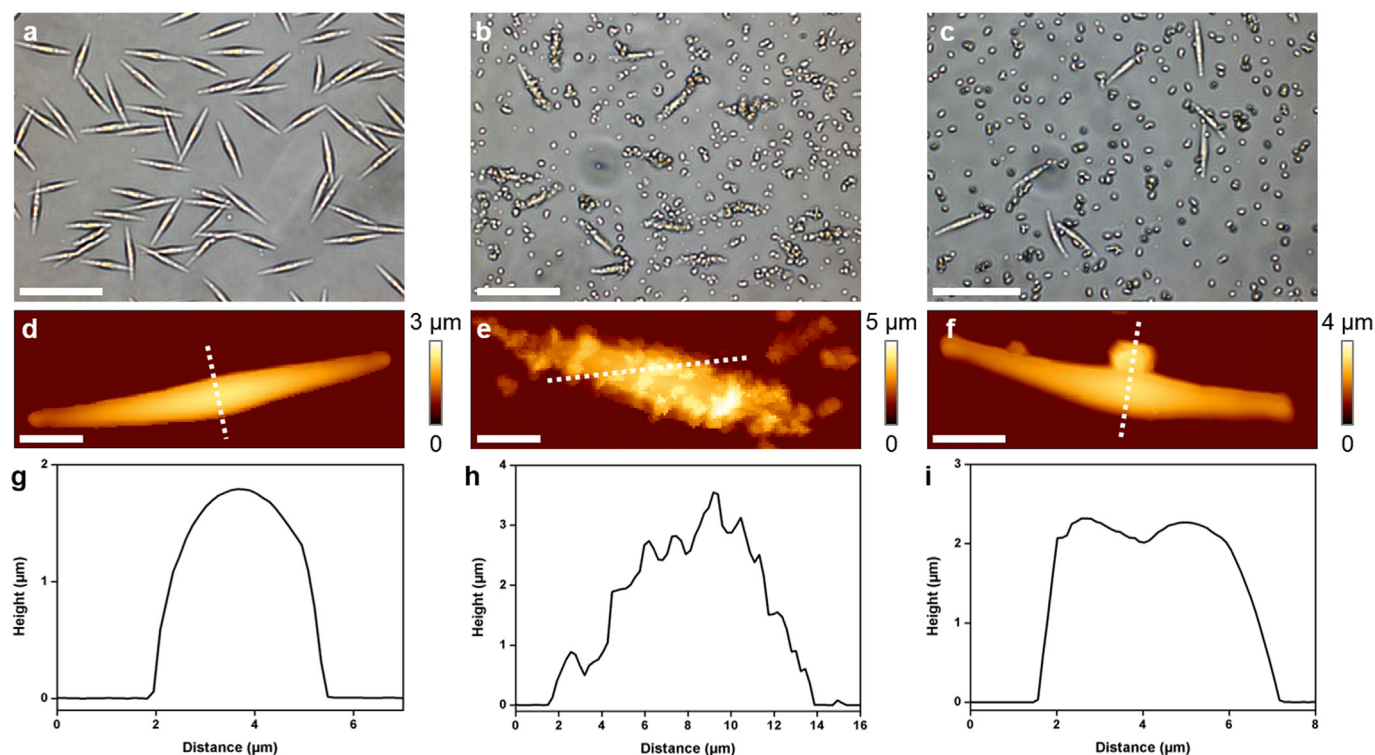


Fig. 3. Effects of flotation on *P. tricornutum* cell surface. (a) Optical image of cells before flotation in sorbitol buffer at pH = 10, or (b) after flotation in sorbitol buffer pH = 10 with Mg(OH)₂ at a concentration of 5.7 mM or (c) with Ca(OH)₂ at a concentration of 10.5 mM. (d) AFM height image of a single *P. tricornutum* cell before flotation, or (e) after flotation in sorbitol buffer pH = 10 with Mg(OH)₂ at a concentration of 5.7 mM or (c) with Ca(OH)₂ at a concentration of 10.5 mM. (g), (h) and (i) are cross-sections taken along the white dashed white lines in respectively (d), (e) and (f). Scale-bars in optical images correspond to 50 μm and to 5 μm in AFM images.

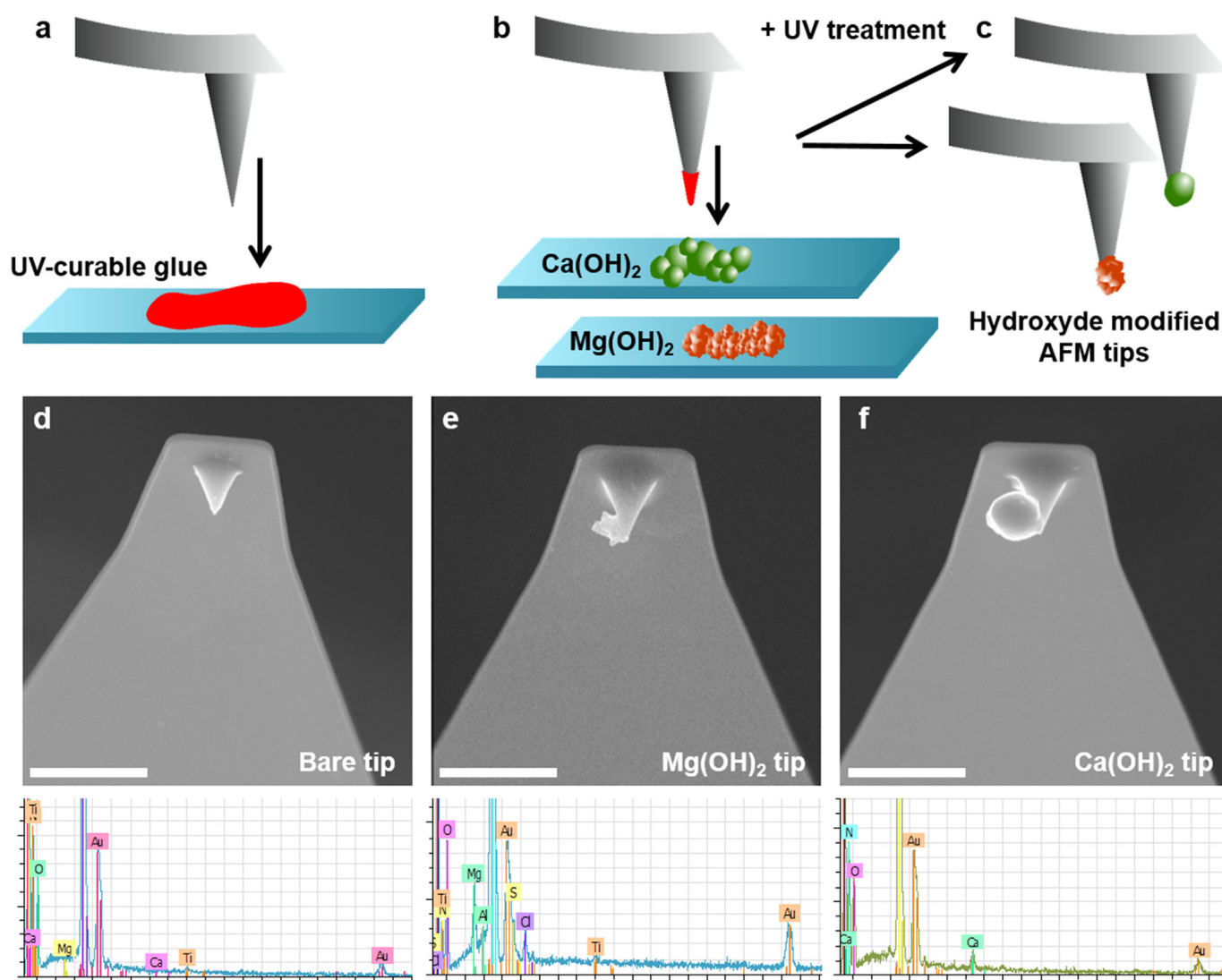


Fig. 4. Functionalization of AFM tips with magnesium or calcium hydroxide particles. (a) to (c) give a schematic representation of the method developed. (a) The end of AFM tips are first covered by a UV-curable glue. (b) Then AFM tips are further put in contact with particles of Ca(OH)_2 or Mg(OH)_2 deposited on a glass surface so that particles attach to the tip. (c) Finally the glue is cured under UV light during 10 min. (d) Scanning electron microscopy image of a bare AFM tip and its corresponding atom spectrum or (e) of a tip functionalized with Mg(OH)_2 particles or (f) of a tip functionalized with Ca(OH)_2 particles. Note on the spectra the peaks corresponding to magnesium and calcium appearing in (e) and (f). Scale-bars in SEM images correspond to 10 μm .

composed of magnesium or calcium atoms, which were not present on bare tips. These experiments allowed then to validate the functionalization strategy that we developed, and show its versatility as different types of inert particles can be functionalized onto tips using this method.

We then used the functionalized tips in multiparametric imaging experiments to characterize and quantify the binding forces between hydroxides particles and living *P. tricornutum* cells at the molecular scale. To this end, cells in sorbitol buffer at a pH of 10 were first probed using multiparametric imaging technology to obtain simultaneous AFM images of the topography and adhesion of the cells (images in Fig. 5). With bare AFM tips, the adhesion image of the cell was dark, meaning that there were no interactions between the tip and the sample (Fig. 5b); the retract force curves then obtained at low scanning speed showed no retract adhesions (Fig. 5c). The same experiments were repeated with Mg(OH)_2 and Ca(OH)_2 functionalized tips; in each case we can see on the height images (Fig. 5 d and g) that the resolution is not as good as when using bare tips, notably on the edges of the cells. This is due to the presence of the particles on the sides of the tips, as seen on SEM images, which reduce their initial sharpening and thus the imaging

resolution. However, both adhesion images (Fig. 5e and h) show adhesion events homogeneously distributed over the entire cell surface; in the case of Mg(OH)_2 tips the adhesion forces seem to be stronger. The retract force curves obtained in each case (Fig. 5f and i) showed typical non-specific retract adhesions, most likely reflecting electrostatic interactions between the negative surface of the cells and the positive surface of both Mg(OH)_2 and Ca(OH)_2 at pH = 10 [35, 36]. Note that in our salt-free buffer, no electrolytes can influence the interactions probed, that are thus only due to the charges brought by the cells and the hydroxides. In the case of Mg(OH)_2 tips, the adhesion force was 109 ± 48 pN (mean \pm SD on a total of $n = 2064$ curves from 12 different cells and 6 different Mg(OH)_2 tips), whereas in the case of Ca(OH)_2 tips, adhesion forces were significantly reduced (p value < 0.05, unpaired t -test) to 95 ± 49 pN (mean \pm SD on a total of $n = 1807$ curves from 12 different cells and 5 different Ca(OH)_2 tips). Therefore, magnesium hydroxide binding to cells is stronger, at pH = 10, than calcium hydroxide. However, both hydroxides adhere to the cells, and through the same type of interactions, thus suggesting that electrostatic binding to cells is not the only mechanism by which Mg(OH)_2 flocculates the cells.

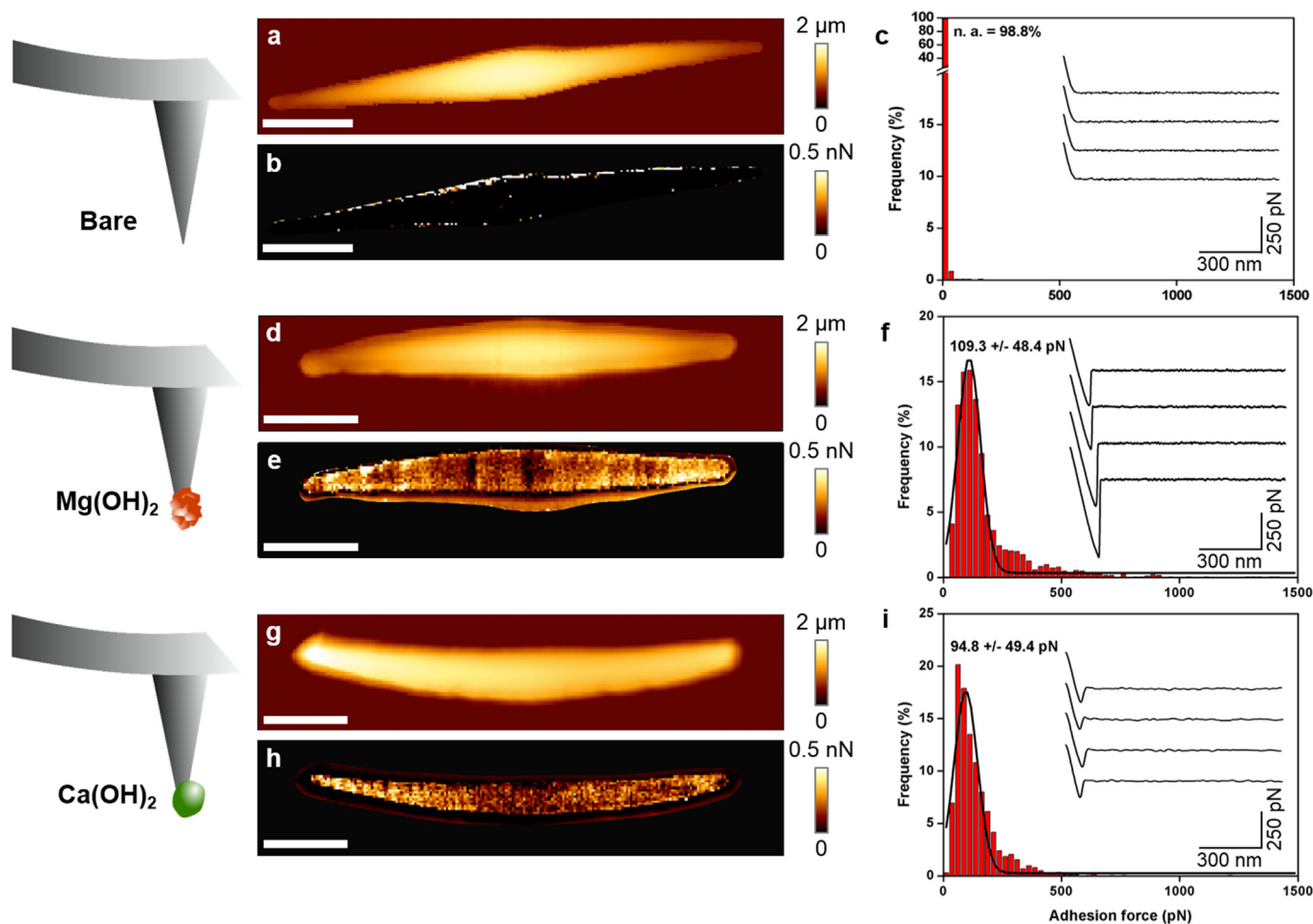


Fig. 5. Probing the interaction between *P. tricornutum* cells and magnesium and calcium hydroxides. (a) AFM height image of a single *P. tricornutum* cell in sorbitol buffer at pH = 10 and (b) corresponding adhesion image, recorded using a bare AFM tip. (c) Histogram representing the adhesion force distribution recorded on cells in sorbitol buffer at pH = 10 with bare AFM tips. (d) AFM height image of a single *P. tricornutum* cell in sorbitol buffer at pH = 10 and (b) corresponding adhesion image, recorded using a Mg(OH)₂ functionalized AFM tip. (f) Histogram representing the adhesion force distribution recorded on cells in sorbitol buffer at pH = 10 with Mg(OH)₂ functionalized AFM tip. (g) AFM height image of a single *P. tricornutum* cell in sorbitol buffer at pH = 10 and (h) corresponding adhesion image, recorded using a Ca(OH)₂ functionalized AFM tip. (i) Histogram representing the adhesion force distribution recorded on cells in sorbitol buffer at pH = 10 with Ca(OH)₂ functionalized AFM tip. The insets in (c), (f) and (i) are representative retract force curves obtained. Scale-bars in AFM images correspond to 5 μm.

4. Discussion

Although flocculation studies involving auto-flocculation [16, 21] or using chemical flocculants [37, 38] have been performed on *P. tricornutum*, there were so far no data on this species harvesting by flotation. Using laboratory-scaled flotation experiments, we have showed that both an increased pH and the alkaline flocculation of the cells play a role in their efficient separation from the water. Using controlled conditions, in pH-adjusted sorbitol buffer, to which hydroxides were directly added in powder, we could determine the effect of each parameter, pH and flocculant, in an independent manner. We then chose to go down to the micro and molecular-scale to precisely understand in what way these parameters were involved in both the attachment of cells to bubbles, and in the formation of flocs, using biophysical approaches. These approaches allow focusing on the cell interface and understand its interactions with its environment, which is a relevant and original approach in biotechnological applications such as flotation. The results we obtained using advanced AFM modes, an innovative tip functionalization method, and zeta potential measurements, allowed us to show how the modification of the cell surface under high pH could participate in both cell-bubble interaction and floc formation, but also to characterize at the molecular scale the interactions between cells and calcium and magnesium hydroxides, thus

providing a molecular foundation for their ability to mediate flocculation.

The cell wall of *P. tricornutum* is composed of three main type of compounds: proteins, lipids and polysaccharides, which follow a complex dynamics depending on the culture conditions or on the morphotype that cell can adopt (fusiform, triradiate or oval) [33]. Francius *et al.* have showed for instance that the cell wall nanomechanical properties of the three different morphotypes were indeed different [29], thus unraveling the link between the composition and architecture of the different compounds in the cell wall and its rigidity. Many studies on the nanomechanical properties of microorganisms, such as yeast, for example, that also have a cell wall composed of proteins and polysaccharides, have showed that external factors could modulate the proportion and architecture of these compounds within the cell wall, and modify its rigidity [39, 40]. In cultures of *P. tricornutum* with no pH control and thus where the pH increases due to the photosynthetic activity of the cells, proteins proportion was lower and replaced by more lipids [33]. Although in our conditions, the timeframe of the experiments might not be enough for the cells to incorporate lipids in the cell wall, it is undeniable that pH has an effect on the composition of the cell wall, and thus on its architecture. Moreover, we have showed that at high pH, the negative cell surface charge is higher, which probably results from the protonation of hydroxyls groups present on

the polysaccharides that compose the cell wall. These changes might then have an impact on the architecture of these components within the cell wall, and thus on the architecture of the cell wall, impacting its rigidity. Therefore the nanomechanical changes that we observe at the two different pH values reflect this cell wall remodeling at an increased pH. But how these nanomechanical changes can be involved in the attachment of cells to bubbles?

The cell wall of microorganisms, from a general point of view, plays several key roles for the cells, such as protection from the environment for example, or maintaining cell shape. Its nanomechanical properties thus have a direct influence on the shape the cell is able to adopt, as Francius and co-workers showed [29], as well as on their deformability. It has been demonstrated in many flotation studies that the shape of the particles had a direct effect on their attachment to the surface of the bubble. For instance, studies have showed that elongated particles had a higher recovery rate than spherical ones in flotation processes [41–43]. Given the lower rigidity of the cells at a pH of 8, it is clear then that in these conditions, cells are more deformable than at pH = 10 and can adopt a more round shape. At increased pH, the rigidity of the cell wall keeps the cell in a rigid fusiform shape compared to pH = 8, which might then have an impact on its interactions with bubbles. This would explain why, at an increased pH, without addition of any flocculants, the removal rate of cells from the water is increased compared to a pH of 8. This effect of pH on the shape of the cells therefore seems to be predominant over the one it has on the charge of the cells; indeed, bubbles in our conditions are negatively charged [15]. Then the increase of the pH making cells more electronegative, the repulsion between cells and bubbles should be more important at increased pH. Nanomechanical data here give a partial explanation on the interactions between cells and bubbles. To go further on this point, a possibility would be to measure directly the interactions between bubbles and cells, at different pH, in order to understand precisely the role of the cell wall in the adhesion to gaz-liquid interfaces.

If the cell wall mechanics seem to have an impact on the interaction with bubbles, it has also a role in the interaction with the hydroxide particles, and thus in floc formation. As we showed in multiparametric imaging experiments using hydroxide modified tips, cells interact through strong electrostatic interactions with both hydroxides. The difference in the adhesion forces between magnesium and calcium hydroxide is perhaps due to the fact that Mg(OH)₂ is able to adhere to the cell surface, as we saw in Fig. 3, whereas Ca(OH)₂ does not. Indeed, while both particles are positively charged, their interactions with the cell wall are different; electrostatics is not the only mechanism involved. Tesson and co-workers showed in a study published in 2008 that Mg(OH)₂ crystals could form a capsule around cells of *P. tricornutum* in cultures at high pH, in line with our observations [44]. According to the authors of this study, this was in fact due to the interactions between magnesium hydroxide and acidic polysaccharides that cells produce under high pH, and which provide surface sites for magnesium hydroxide biosorption. However in this study, cells were cultured with no pH control and analyzed right away: in our case, cells are washed before all experiments, which must probably remove the potentially excreted polysaccharides from the cells surface, as it is the case for other microorganisms [45]. Indeed, in experiments performed in these conditions, at pH = 10, using AFM tips functionalized with a lectin that binds to polysaccharides (concanavalin A), we could not pull any molecules from the surface, indicating thus the absence of these polysaccharides (data not showed). Therefore there might be another mechanism involved in the adhesion of only magnesium hydroxide into the cell wall. Perhaps the size of the particles could be an explanation: on AFM images and cross-sections in Fig. 3, we can clearly see that Mg(OH)₂ particles have a size around 1 μm, while Ca(OH)₂ particles are bigger with a size of approximately 2 μm. It is then possible that calcium hydroxide particles are too big to be coated on the cell wall. Another possibility could rely in a specificity of proteins present at the surface for magnesium. Willis et al. have started to identify proteins

expressed at the surface of *P. tricornutum* cells involved in cell adhesion [46]; perhaps one of these proteins has a specific binding site for magnesium hydroxide. But what must be remembered is that the interaction between magnesium hydroxide and the cell wall of *P. tricornutum* relies on several mechanisms, among which one is based on electrostatic interactions, as showed in our force spectroscopy experiments.

The Mg(OH)₂ capsule that forms around the cells seems to be involved in flocculation of the cells. Indeed, when magnesium hydroxide is used as a flocculant, better removal rates are reached in our flocculation/flotation system. In different studies the team of Muylaert has established that the flocculation of cells mediated by Mg(OH)₂ was based on a charge neutralization mechanism. In this mechanism, the positive charges of the hydroxide particles strongly interact and neutralize the negative ones of the cells. As a result, the electrostatic repulsion between the cells disappear and cells flocculate [16, 47]. If flocculation was only relying on this mechanism, then when using Ca(OH)₂, also positively charged and strongly interacting with the cells, better flocculation rates should be reached. Another mechanism that can be involved in flocculation is called the sweeping mechanism, where the cells are entrapped in a massive precipitation [47–49]. Although the interactions that we measure in this study, between hydroxide particles and cells, are probably involved in this type of mechanism, the fact that hydroxides are added to the cell suspension in buffer, and not formed *in situ*, then prevent this mechanism to happen in our experimental conditions. Thus not only the interaction, but the absorption of the hydroxide particles have a role in the flocculation of the cells.

Altogether, the biophysical data that we obtain here in this study, provide new insights into both the processes of cell-bubble interaction and floc formation, involved in the flocculation/flotation mechanism of *P. tricornutum*. The nanomechanical properties of the cell wall of cells, obtained using AFM nanoindentation measurements at different pH, suggest that the shape of the particles is involved in their interactions with bubbles and thus give an explanation for the better flotation efficiencies obtained with only an increased pH. Concerning floc formation, zeta potential measurements, AFM imaging and force spectroscopy data obtained using particle-functionalized AFM tips show that this process rely on both a charge neutralization process, but also on the absorption of hydroxide particles into the cell wall of *P. tricornutum*. This explains thus why when Mg(OH)₂ is used as a flocculant, better separation rates are reached in flotation experiments, as its ability to form a capsule around cells seem to be involved in the successful formation of flocs.

5. Conclusions

In conclusion, our results demonstrate that charge neutralization is not the only mechanism underlying flocculation by magnesium hydroxide. They also highlight the unexpected role of the cell wall in both flocculation and flotation. Indeed, while its nanomechanical properties are involved in its interaction with bubbles, its surface charge is essential for interacting with hydroxide particles through electrostatic interactions. It also features the ability of adhering of magnesium hydroxide particles, which, as our study shows, is a key point for mediating flocculation and thus further flotation. The magnesium-hydroxide flocculation/flotation mechanism is thus a two-partner system; both the changes undertaken by the cell wall and the interactions with hydroxide particles are needed to successfully flocculate and harvest the cells by flotation. However, despite the new insights provided by our study, still some information are missing in order to fully understand the flocculation/flotation mechanism of *P. tricornutum*: further studies will thus focus on the interactions between cells and bubbles that are for the moment not characterized. For that, perspective work will include force spectroscopy experiments between cells, in the presence of hydroxide particles or not, and bubbles, at different pH. This

will help elucidating the mechanisms, at the molecular and cellular scale, involved in flotation process, and perhaps reveal the influence of floc formation on bubble attachment. But for the moment, the new information that this study provides may open up new ways to improve and optimize microalgae harvesting by flotation; by controlling auto-flocculation mechanisms, flotation efficiency could be increased without adding any flocculants, thus reducing the toxicity and costs in biotechnological applications such as biofuel production. Moreover, the fundamental knowledge produced here, but also the multi-scale approach developed provide a new base to study and understand other environmentally-significant mechanisms in which microalgae flocculation is involved, such as for example biofilm [50] or marine snow [51] formation that take place in marine environments.

Acknowledgements

C. F.-D. is a postdoctoral researcher supported by the AgreeSkills fellowship programme, which has received funding from the EU's Seventh Framework Programme under grant agreement No. FP7-609398 (AgreeSkills + contract).

Author contribution

C. F.-D. and P. G. conceived the project. C. F.-D. designed the experiments. C. F.-D. and V. G. performed the experiments. C. F.-D., M. C., F. D. and P. G. discussed and interpreted the results. C. F.-D. wrote the initial manuscript. C. F.-D., M. C., F. D. and P. G. reviewed and contributed to the manuscript. All authors approved the manuscript.

Declarations

- The authors declare that they have no competing interests
- No conflicts, informed consent, human or animal rights applicable
- All authors agree to authorship and submission of the manuscript for peer review

References

- [1] P.G. Falkowski, R.T. Barber, V.V. Smetacek, Biogeochemical controls and feedbacks on ocean primary production, *Science* 281 (1998) 200–207.
- [2] S. Scala, C. Bowler, Molecular insights into the novel aspects of diatom biology, *Cell. Mol. Life Sci.* 58 (2001) 1666–1673, <http://dx.doi.org/10.1007/PL00000804>.
- [3] T. Lebeau, J.-M. Robert, Diatom cultivation and biotechnologically relevant products. Part II: current and putative products, *Appl. Microbiol. Biotechnol.* 60 (2003) 624–632, <http://dx.doi.org/10.1007/s00253-002-1177-3>.
- [4] T.C. Adame-Vega, D.K.Y. Lim, M. Timmins, F. Vernen, Y. Li, P.M. Schenk, Microalgal biofactories: a promising approach towards sustainable omega-3 fatty acid production, *Microb. Cell Factories* 11 (2012) 96, <http://dx.doi.org/10.1186/1475-2859-11-96>.
- [5] N.F. Santos-Sánchez, R. Valadez-Blanco, B. Hernández-Carlos, A. Torres-Ariño, P.C. Guadarrama-Mendoza, R. Salas-Coronado, Lipids rich in ω -3 polyunsaturated fatty acids from microalgae, *Appl. Microbiol. Biotechnol.* 100 (2016) 8667–8684, <http://dx.doi.org/10.1007/s00253-016-7818-8>.
- [6] F. Daboussi, S. Leduc, A. Maréchal, G. Dubois, V. Guyot, C. Perez-Michaut, A. Amato, A. Falcatoire, A. Juillerat, M. Beurdeley, D.F. Voytas, L. Cavarec, P. Duchateau, Genome engineering empowers the diatom *Phaeodactylum tricoratum* for biotechnology, *Nat. Commun.* 5 (2014) 3831, <http://dx.doi.org/10.1038/ncomms4831>.
- [7] L.-J. Dolch, E. Maréchal, Inventory of fatty acid desaturases in the pennate diatom *Phaeodactylum tricoratum*, *Mar. Drugs* 13 (2015) 1317–1339, <http://dx.doi.org/10.3390/md13031317>.
- [8] E. Waltz, Biotech's green gold? *Nat. Biotechnol.* 27 (2009) 15–18, <http://dx.doi.org/10.1038/nbt0109-15>.
- [9] T. Ndikubwimana, J. Chang, Z. Xiao, W. Shao, X. Zeng, I.-S. Ng, Y. Lu, Flotation: a promising microalgae harvesting and dewatering technology for biofuels production, *Biotechnol. J.* 11 (2016) 315–326, <http://dx.doi.org/10.1002/biot.201500175>.
- [10] M.K. Lam, K.T. Lee, Microalgae biofuels: a critical review of issues, problems and the way forward, *Biotechnol. Adv.* 30 (2012) 673–690, <http://dx.doi.org/10.1016/j.biotechadv.2011.11.008>.
- [11] E. Molina Grima, E.-H. Belarbi, F.G. Ación Fernández, A. Robles Medina, Y. Chisti, Recovery of microalgal biomass and metabolites: process options and economics, *Biotechnol. Adv.* 20 (2003) 491–515, [http://dx.doi.org/10.1016/S0734-9750\(02\)00050-2](http://dx.doi.org/10.1016/S0734-9750(02)00050-2).
- [12] N. Uduman, Y. Qi, M.K. Danquah, G.M. Forde, A. Hoadley, Dewatering of micro-algal cultures: a major bottleneck to algae-based fuels, *J. Renewable Sustainable Energy* 2 (2010) 012701, <http://dx.doi.org/10.1063/1.3294480>.
- [13] S. Garg, Y. Li, L. Wang, P.M. Schenk, Flotation of marine microalgae: effect of algal hydrophobicity, *Bioresour. Technol.* 121 (2012) 471–474, <http://dx.doi.org/10.1016/j.biortech.2012.06.111>.
- [14] S. Garg, L. Wang, P.M. Schenk, Effective harvesting of low surface-hydrophobicity microalgae by froth flotation, *Bioresour. Technol.* 159 (2014) 437–441, <http://dx.doi.org/10.1016/j.biortech.2014.03.030>.
- [15] C. Yang, T. Dabros, D. Li, J. Czarnecki, J.H. Masliyah, Measurement of the zeta potential of gas bubbles in aqueous solutions by microelectrophoresis method, *J. Colloid Interface Sci.* 243 (2001) 128–135, <http://dx.doi.org/10.1006/jcis.2001.7842>.
- [16] S. Lama, K. Muylaert, T.B. Karki, I. Foubert, R.K. Henderson, D. Vandamme, Flocculation properties of several microalgae and a cyanobacterium species during ferric chloride, chitosan and alkaline flocculation, *Bioresour. Technol.* 220 (2016) 464–470, <http://dx.doi.org/10.1016/j.biortech.2016.08.080>.
- [17] A. Schlesinger, D. Eisenstadt, A. Bar-Gil, H. Carmely, S. Einbinder, J. Gressel, Inexpensive non-toxic flocculation of microalgae contradicts theories; overcoming a major hurdle to bulk algal production, *Biotechnol. Adv.* 30 (2012) 1023–1030, <http://dx.doi.org/10.1016/j.biotechadv.2012.01.011>.
- [18] A. Sukenik, G. Shelef, Algal autoflocculation—verification and proposed mechanism, *Biotechnol. Bioeng.* 26 (1984) 142–147, <http://dx.doi.org/10.1002/bit.260260206>.
- [19] A. Besson, P. Guiraud, High-pH-induced flocculation-flotation of the hypersaline microalga *Dunaliella salina*, *Bioresour. Technol.* 147 (2013) 464–470, <http://dx.doi.org/10.1016/j.biortech.2013.08.053>.
- [20] Z. Wu, Y. Zhu, W. Huang, C. Zhang, T. Li, Y. Zhang, A. Li, Evaluation of flocculation induced by pH increase for harvesting microalgae and reuse of flocculated medium, *Bioresour. Technol.* 110 (2012) 496–502, <http://dx.doi.org/10.1016/j.biortech.2012.01.101>.
- [21] D. Vandamme, P.I. Pohl, A. Beuckels, I. Foubert, P.V. Brady, J.C. Hewson, K. Muylaert, Alkaline flocculation of *Phaeodactylum tricoratum* induced by brucite and calcite, *Bioresour. Technol.* 196 (2015) 656–661, <http://dx.doi.org/10.1016/j.biortech.2015.08.042>.
- [22] G. Binnig, C.F. Quate, C. Gerber, Atomic force microscope, *Phys. Rev. Lett.* 56 (1986) 930–934.
- [23] C. Formosa-Dague, R.E. Duval, E. Dague, Cell biology of microbes and pharmacology of antimicrobial drugs explored by atomic force microscopy, *Semin. Cell Dev. Biol.* 73 (2018) 165–173, <http://dx.doi.org/10.1016/j.semcdb.2017.06.022>.
- [24] L. Chopinet, C. Formosa, M.P. Rols, R.E. Duval, E. Dague, Imaging living cells surface and quantifying its properties at high resolution using AFM in QI™ mode, *Micron Oxf. Engl.* 1993 (48) (2013) 26–33, <http://dx.doi.org/10.1016/j.micron.2013.02.003>.
- [25] C. Formosa, M. Schiavone, A. Boisrame, M.L. Richard, R.E. Duval, E. Dague, Multiparametric imaging of adhesive nanodomains at the surface of *Candida albicans* by atomic force microscopy, *Nanomedicine* 11 (2015) 57–65, <http://dx.doi.org/10.1016/j.nano.2014.07.008>.
- [26] C. Formosa-Dague, P. Speziale, T.J. Foster, J.A. Geoghegan, Y.F. Dufrière, Zinc-dependent mechanical properties of *Staphylococcus aureus* biofilm-forming surface protein SasG, *Proc. Natl. Acad. Sci.* 113 (2016) 410–415, <http://dx.doi.org/10.1073/pnas.1519265113>.
- [27] Q.K. Ong, I. Sokolov, Attachment of nanoparticles to the AFM tips for direct measurements of interaction between a single nanoparticle and surfaces, *J. Colloid Interface Sci.* 310 (2007) 385–390, <http://dx.doi.org/10.1016/j.jcis.2007.02.010>.
- [28] R.R.L. Guillard, Culture of phytoplankton for feeding marine invertebrates, in: W.L. Smith, M.H. Chanley (Eds.), *Culture of Marine Invertebrate Animals*, Plenum Press, New York, 1975, pp. 29–60.
- [29] G. Francius, B. Tesson, E. Dague, V. Martin-Jézéquel, Y.F. Dufrière, Nanostructure and nanomechanics of live *Phaeodactylum tricoratum* morphotypes, *Environ. Microbiol.* 10 (2008) 1344–1356, <http://dx.doi.org/10.1111/j.1462-2920.2007.01551.x>.
- [30] H. Hertz, Ueber die berührung fester elastischer körper, *J. Reine Angew. Math.* (1881) 156–171.
- [31] J.L. Hutter, J. Bechhoefer, Calibration of atomic-force microscope tips, *Rev. Sci. Instrum.* 64 (1993) 1868–1873.
- [32] S. Feng, C. Bagia, G. Mpourmpakis, Determination of proton affinities and acidity constants of sugars, *J. Phys. Chem. A* 117 (2013) 5211–5219, <http://dx.doi.org/10.1021/jp403355e>.
- [33] B. Tesson, M.J. Genet, V. Fernandez, S. Degand, P.G. Rouxhet, V. Martin-Jézéquel, Surface chemical composition of diatoms, *Chembiochem Eur. J. Chem. Biol.* 10 (2009) 2011–2024, <http://dx.doi.org/10.1002/cbic.200800811>.
- [34] I. Sokolov, S. Iyer, C.D. Woodworth, Recovery of elasticity of aged human epithelial cells in vitro, *Nanomedicine* 2 (2006) 31–36, <http://dx.doi.org/10.1016/j.nano.2005.12.002>.
- [35] W. Gu, D.W. Bousfield, C.P. Tripp, Formation of calcium carbonate particles by direct contact of Ca(OH)₂ powders with supercritical CO₂, *J. Mater. Chem.* 16 (2006) 3312–3317, <http://dx.doi.org/10.1039/B607184H>.
- [36] J.X. Lin, L. Wang, Adsorption of dyes using magnesium hydroxide-modified diatomite, *Desal. Water Treat.* 8 (2009) 263–271, <http://dx.doi.org/10.5004/dwt.2009.786>.
- [37] H. Zheng, Z. Gao, J. Yin, X. Tang, X. Ji, H. Huang, Harvesting of microalgae by flocculation with poly (γ -glutamic acid), *Bioresour. Technol.* 112 (2012) 212–220, <http://dx.doi.org/10.1016/j.biortech.2012.02.086>.
- [38] G.P. 't Lam, M.H. Vermuë, G. Olivieri, L.a.M. van den Broek, M.J. Barbosa, M.H.M. Eppink, R.H. Wijffels, D.M.M. Kleinegris, Cationic polymers for successful

- flocculation of marine microalgae, *Bioresour. Technol.* 169 (2014) 804–807, <http://dx.doi.org/10.1016/j.biortech.2014.07.070>.
- [39] E. Dague, R. Bitar, H. Ranchon, F. Durand, H.M. Yken, J.M. François, An atomic force microscopy analysis of yeast mutants defective in cell wall architecture, *Yeast* 27 (2010) 673–684, <http://dx.doi.org/10.1002/yea.1801>.
- [40] C. Formosa, M. Schiavone, H. Martin-Yken, J.M. François, R.E. Duval, E. Dague, Nanoscale effects of Caspofungin against two yeast species, *Saccharomyces cerevisiae* and *Candida albicans*, *Antimicrob. Agents Chemother.* 57 (2013) 3498–3506, <http://dx.doi.org/10.1128/AAC.00105-13>.
- [41] M. Yekeler, U. Ulusoy, C. Hıçyılmaz, Effect of particle shape and roughness of talc mineral ground by different mills on the wettability and floatability, *Powder Technol.* 140 (2004) 68–78, <http://dx.doi.org/10.1016/j.powtec.2003.12.012>.
- [42] P.T.L. Koh, F.P. Hao, L.K. Smith, T.T. Chau, W.J. Bruckard, The effect of particle shape and hydrophobicity in flotation, *Int. J. Miner. Process.* 93 (2009) 128–134, <http://dx.doi.org/10.1016/j.minpro.2009.07.007>.
- [43] D.I. Verrelli, W.J. Bruckard, P.T.L. Koh, M.P. Schwarz, B. Follink, Particle shape effects in flotation. Part 1: microscale experimental observations, *Miner. Eng.* 58 (2014) 80–89, <http://dx.doi.org/10.1016/j.mineng.2014.01.004>.
- [44] B. Tesson, C. Gaillard, V. Martin-Jézéquel, Brucite formation mediated by the diatom *Phaeodactylum tricornutum*, *Mar. Chem.* 109 (2008) 60–76, <http://dx.doi.org/10.1016/j.marchem.2007.12.005>.
- [45] C. Formosa-Dague, C. Feuillie, A. Beaussart, S. Derclaye, S. Kuchariková, I. Lasa, P. Van Dijck, Y.F. Dufrene, Sticky matrix: adhesion mechanism of the staphylococcal polysaccharide intercellular adhesin, *ACS Nano* 10 (2016) 3443–3452, <http://dx.doi.org/10.1021/acs.nano.5b07515>.
- [46] A. Willis, M. Eason-Hubbard, O. Hodson, U. Maheswari, C. Bowler, R. Wetherbee, Adhesion molecules from the diatom *Phaeodactylum tricornutum* (Bacillariophyceae): genomic identification by amino-acid profiling and in vivo analysis, *J. Phycol.* 50 (2014) 837–849, <http://dx.doi.org/10.1111/jpy.12214>.
- [47] D. Vandamme, I. Foubert, K. Muylaert, Flocculation as a low-cost method for harvesting microalgae for bulk biomass production, *Trends Biotechnol.* 31 (2013) 233–239, <http://dx.doi.org/10.1016/j.tibtech.2012.12.005>.
- [48] P.V. Brady, P.I. Pohl, J.C. Hewson, A coordination chemistry model of algal auto-flocculation, *Algal Res.* 5 (2014) 226–230, <http://dx.doi.org/10.1016/j.algal.2014.02.004>.
- [49] J. Phasey, D. Vandamme, H.J. Fallowfield, Harvesting of algae in municipal wastewater treatment by calcium phosphate precipitation mediated by photosynthesis, sodium hydroxide and lime, *Algal Res.* 27 (2017) 115–120, <http://dx.doi.org/10.1016/j.algal.2017.06.015>.
- [50] H. Dang, C.R. Lovell, Microbial surface colonization and biofilm development in marine environments, *Microbiol. Mol. Biol. Rev.* 80 (2015) 91–138, <http://dx.doi.org/10.1128/MMBR.00037-15>.
- [51] B. Tansel, Morphology, composition and aggregation mechanisms of soft bioflocs in marine snow and activated sludge: a comparative review, *J. Environ. Manag.* 205 (2018) 231–243, <http://dx.doi.org/10.1016/j.jenvman.2017.09.082>.